

OmniV-Med: Scaling Medical Vision-Language Model for Universal Visual Understanding

Songtao Jiang¹, Yuan Wang¹, Sib0 Song², Yan Zhang¹, Zijie Meng¹,
Bohan Lei¹, Jian Wu¹, Jimeng Sun³, Zuozhu Liu^{1†}
¹Zhejiang University ²Alibaba Group ³UIUC

Abstract

The practical deployment of medical vision-language models (Med-VLMs) necessitates seamless integration of textual data with diverse visual modalities, including 2D/3D images and videos, yet existing models typically employ separate encoders for different modalities. To address this limitation, we present OmniV-Med, a unified framework for multimodal medical understanding. Our technical contributions are threefold: First, we construct OmniV-Med-Instruct, a comprehensive multimodal medical dataset containing 252K instructional samples spanning 14 medical image modalities and 11 clinical tasks. Second, we devise a rotary position-adaptive encoder that processes multi-resolution 2D/3D images and videos within a unified architecture, diverging from conventional modality-specific encoders. Third, we introduce a medical-aware token pruning mechanism that exploits spatial-temporal redundancy in volumetric data (e.g., consecutive CT slices) and medical videos, effectively reducing 60% of visual tokens without performance degradation. Empirical evaluations demonstrate that OmniV-Med-7B achieves state-of-the-art performance on 7 benchmarks spanning 2D/3D medical imaging and video understanding tasks. Notably, our lightweight variant (OmniV-Med-1.5B) attains comparable performance while requiring only 8 RTX3090 GPUs for training and supporting efficient long-video inference. Data, code and model will be released.

1 Introduction

The unified understanding and generation of textual and visual inputs is pivotal for advancing next-generation vision-language models (VLMs) (Bordes et al., 2024; Bai et al., 2023; Wu et al., 2024; Zhan et al., 2024b; Zhang et al., 2025). Recent progress in multimodal VLMs has demon-

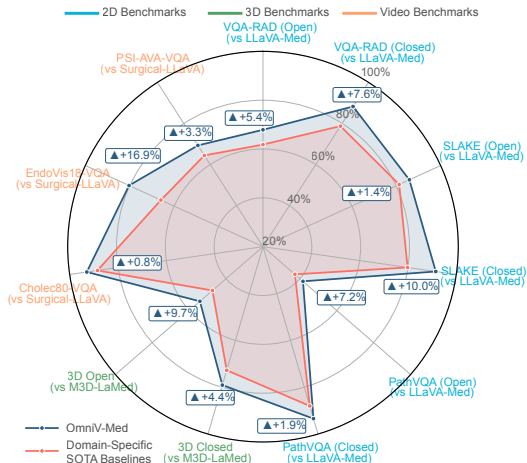


Figure 1: Comparison with state-of-the-art methods on medical 2D/3D image and video benchmarks.

strated promising results, with frameworks leveraging unified tokenizers or specialized encoders to process heterogeneous inputs (e.g., images, text, audio, and video) (Wu et al., 2023c; Zhan et al., 2024a; Li et al., 2024c). In the medical domain, emerging works such as LLaVA-Med, RadFM, and PathChat (Li et al., 2024b; Wu et al., 2023a; Lu et al., 2024; Xu et al., 2024) have extended these capabilities to medical vision-language tasks. However, existing approaches either focus on domain-specific image interpretation (Zhou et al., 2023; Jiao et al., 2023; Jiang et al., 2024c; Moor et al., 2023b; Li et al., 2024b), or are restricted to radiology-specific 2D/3D imaging analysis (Wu et al., 2023a). This fragmentation limits their ability to holistically process multimodal visual data with textual instructions (e.g., integrating endoscopic video, 3D CT scans and 2D images), thereby hindering deployment in complex real-world scenarios such as AI-assisted surgery and adaptive treatment planning (Bodenstedt et al., 2020; Wang et al., 2023; Zhang et al., 2024).

Developing a unified Med-VLM model capable of processing diverse multimodal inputs poses

† Corresponding author: zuozhuliu@intl.zju.edu.cn

three fundamental challenges. First, the medical domain lacks robust encoders tailored for 3D volumetric data and temporal videos (Wang et al., 2022; Nwoye et al., 2023), compounded by the absence of unified encoders capable of simultaneously modeling both modalities. Discrepancies among 2D/3D spatial structures and temporal video dynamics, along with limited high-quality medical datasets, pose significant challenges in achieving robust alignment of cross-modal representation (He et al., 2024; Ren et al., 2024). Second, widely-used encoders like CLIP-ViT (Radford et al., 2021), which rely on fixed positional embeddings, struggle to adapt to the diverse spatial resolutions (e.g., gigapixel pathology slides) and temporal dynamics in medical videos. Additionally, existing tokenization strategies for medical 3D volumes and videos are inefficient and lack scalability (Hirsch et al., 2023). Although techniques such as bilinear interpolation (Li et al., 2024a; Kirkland and Kirkland, 2010) have been used in general domains to mitigate this issue, they often fail to preserve the fine-grained details essential for medical analysis. Third, the medical domain suffers from a severe shortage of instruction-aligned datasets for 3D and video modalities. The lack of large-scale, task-specific training data hinders the development of models capable of robust multimodal alignment and domain-adaptive reasoning, limiting their practical utility in clinical settings.

In this paper, we propose **OmniV-Med**, a unified Med-VLM foundation model for processing medical text, 2D/3D images, and medical videos. We first construct **OmniV-Med-Instruct**, a comprehensive instruction-following dataset spanning 14 medical (e.g., 2D single/multi-image, 3D volumetric, and video data) with 252K vision-language samples. For the model architecture, unlike prior methods that rely on modality-specific encoders (Li et al., 2023; Lin et al., 2023), we design a single vision encoder leveraging a rotary position-adaptive encoding strategy (Dehghani et al., 2023) to unify 2D, 3D, and video processing. Our encoder first learns relative spatial relationships between patches in 2D images (height/width dimensions) and extrapolates these positional encodings to the third dimension: 1) 3D images are treated as multi-view slices with spatial position encoding, and 2) videos are modeled as multi-frame sequences with temporal position encoding. This contrasts with conventional approaches that simply concatenate fixed positional embeddings for multi-image 3D/video

inputs, lacking explicit spatiotemporal modeling. Furthermore, we adopt a progressive strategy: the model is first pretrained on high-quality 2D vision-language pairs, then extended to 3D and video data using spatiotemporal extrapolation. This progressive training enables emergent capabilities, facilitating fast and effective cross-modal alignment by projecting all modalities into a unified latent space.

To reduce computational overheads, we introduce a medical-aware token pruning strategy that dynamically compresses redundant tokens during training and inference. By computing $L - 1$ distances between patch of consecutive video frames or adjacent 3D slices, we prune tokens with differences below a predefined threshold (Choudhury et al., 2024). This encourages the model to prioritize significant frame-to-frame and cross-view variations, demonstrating satisfactory trade-off between performance and computational efficiency.

Our method surpasses state-of-the-art (SoTA) task-specific models across 7 widely-used medical vision-language benchmarks across 2D/3D images and videos. For 2D medical visual question answering (VQA), we evaluate on both close- and open-end tasks in Rad-VQA (Lau et al., 2018), SLAKE (Liu et al., 2021), and PathVQA (He et al., 2020). For 3D tasks, we assess performance on the latest M3D-VQA (Bai et al., 2024), covering both close- and open-ended VQA tasks. For medical video, we evaluate on the Cholec80-VQA (Seenivasan et al., 2022), PSI-AVA-VQA (Valderrama et al., 2022), and EndoVis18-VQA (Seenivasan et al., 2023). Our OmniV-Med establishes SoTA performance on all 7 benchmarks with **OmniV-Med-7B**. Our lightweight version, **OmniV-Med1.5B**, achieves competitive performance while requiring only $8 \times$ RTX 3090 GPUs for training, matching or even surpassing SoTA models in individual tasks. To our knowledge, this work presents the first Med-VLM unifying text, 2D/3D images, and videos within a single framework, offering a scalable and practical solution for real-world clinical workflows.

2 OmniV-Med

2.1 OmniV-Med-Instruct Construction

The coverage of data modalities, sample sizes, tasks and statistics in OmniV-Med-Instruct are illustrated in Figure 2. Our dataset covers 14 imaging modalities for various diseases, including regular images such as CT, MRI, X-ray, and

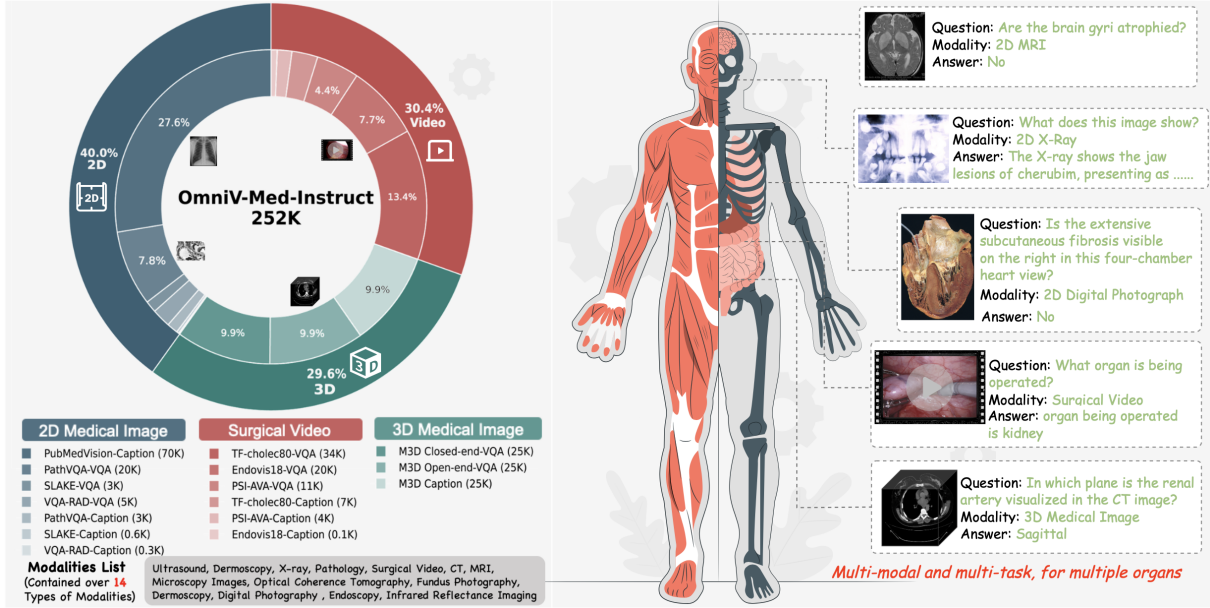


Figure 2: Data distribution, coverage and examples of OmniV-Med-Instruct.

pathology, and domain-specific images such as dermoscopy and endoscopy. For 2D-VL instructions, we curated mainstream medical datasets on two major tasks: Medical VQA (Med-VQA) and Medical Report Generation (MRG), including Rad-VQA (Lau et al., 2018), MIMIC-CXR (Bae et al., 2024), SLAKE (Liu et al., 2021), and PathVQA (He et al., 2020). To enhance the model’s instruction-following capabilities, we also sampled 70K instruction-following examples from PubMedVision (Chen et al., 2024). For 3D-VL pairs, we sampled 75K data points from the M3D datasets (Bai et al., 2024), which cover diverse 3D medical tasks such as image-text retrieval, MRG, VQA, and positioning.

For medical video-language pairs, we leveraged existing VLMs to build the an open-source medical video instruction-following dataset. First, we created video VQA tasks using datasets including Cholec80 (Seenivasan et al., 2022), PSI-AVA (Valderrama et al., 2022), and EndoVis18 (Seenivasan et al., 2023), which cover various surgical procedures. We formed short video segments from consecutive frames and their original VQA questions and answers, allowing the model to learn from continuous video sequences. For video captioning tasks, due to the absence of open-source medical-specific video VLMs, we used the general Qwen2.5-VL-72B (Bai et al., 2025) to generate captions by combining frame-level QA texts with their corresponding video segments. To ensure data quality, we applied rejection

sampling (Touvron et al., 2023) to filter out high-quality video-text pairs (see details in Figure 4).

2.2 Training Pipeline

Our training process consists of three stages: 1) 2D Med-VL alignment, enhancing the model’s understanding of 2D medical images with VL caption pairs; 2) medical instruction-following tuning, enabling the model to follow complex instructions based on medical image understanding; and 3) medical mixed-modal tuning, improving model’s capacity to interpret diverse spatial and temporal VL inputs.

2D Med-VL Alignment. In stage 1, we align medical vision and language inputs using 647K image-caption pairs from PubMedVision_Alignment (Chen et al., 2024). We freeze the LLM backbone and fine-tune the pre-trained SigLIP (Zhai et al., 2023) along with the MLP projector as the vision encoder. To better handle different image resolutions, we replace the original fixed position embedding in SigLIP with a rotary position embedding, creating the *rotary position-adaptive encoder*. The rotary position embedding is defined as:

$$\mathbf{R}_{\theta,d} = \begin{pmatrix} \cos \theta & -\sin \theta \\ \sin \theta & \cos \theta \end{pmatrix}, \quad (1)$$

where θ represents the rotation angle and d denotes the embedding dimension. For a given position m , the rotary embedding is applied to the query \mathbf{q}_m

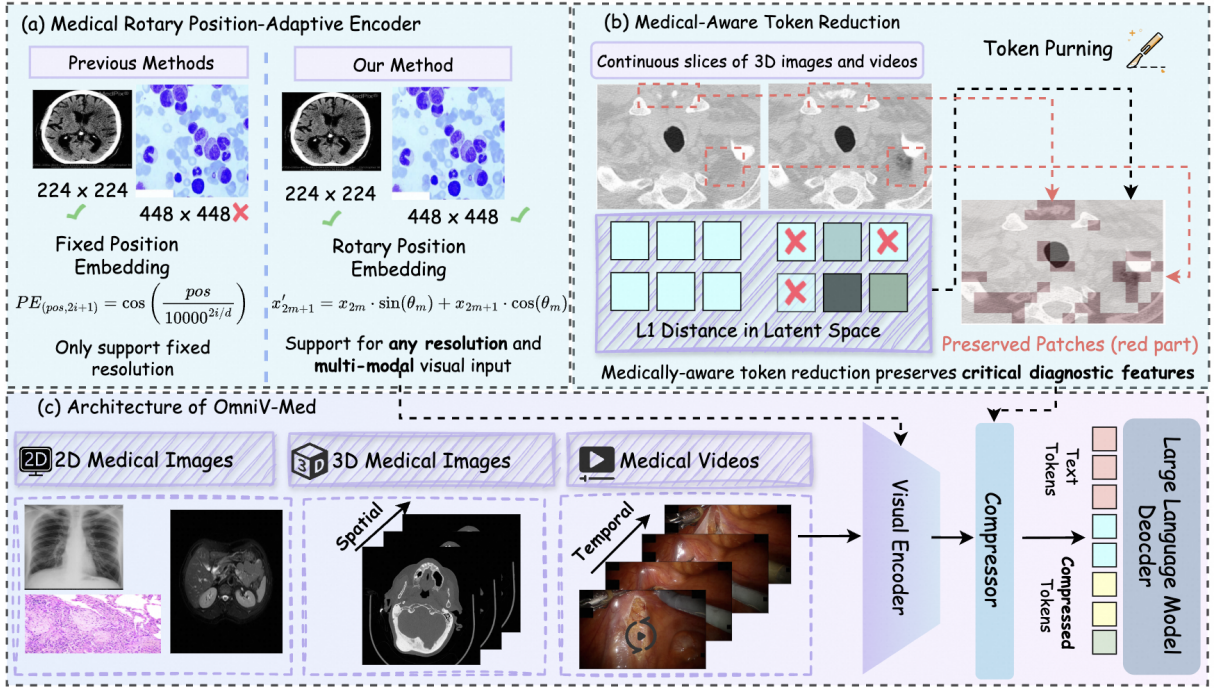


Figure 3: OmniV-Med framework consists of three key components: (a). a medical rotary position-adaptive encoder supporting various multi- modalities with different resolutions, (b). medical-aware token reduction to efficiently handle redundant frames and slices in videos and 3D images, and (c). the architecture of our OmniV-Med model.

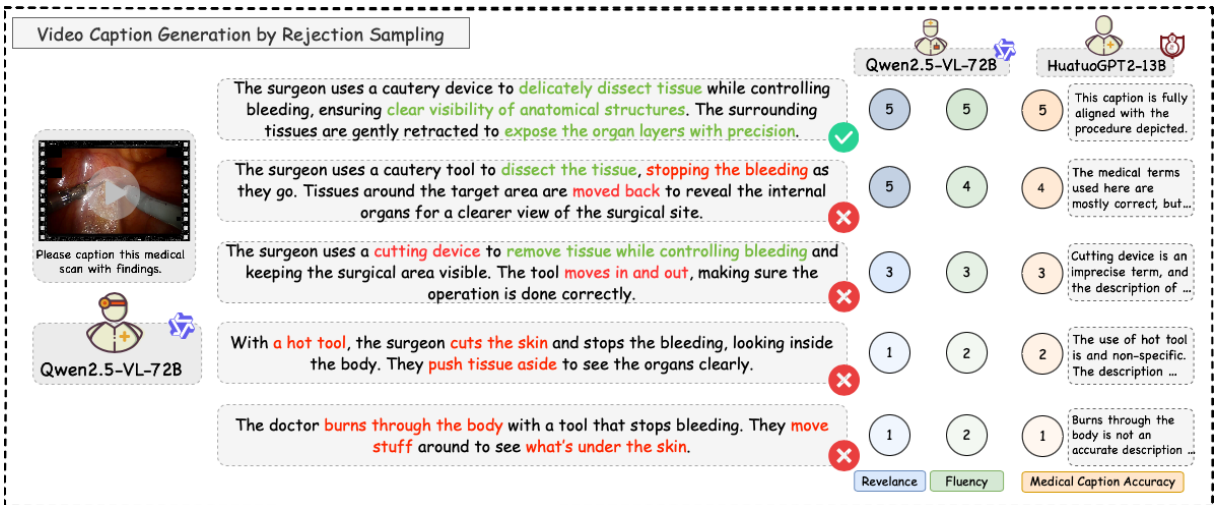


Figure 4: A framework for high-quality medical video captioning via rejection sampling: Utilizing Qwen2.5-VL-72B for candidate generation and combining Qwen2.5-VL-72B with HuatuoGPT2-13B for medical caption evaluation based on relevance, fluency, and accuracy (5-point scale).

and key \mathbf{k}_n vectors as:

$$\mathbf{q}'_m = \mathbf{R}_{\theta,d}(m)\mathbf{q}_m, \quad \mathbf{k}'_n = \mathbf{R}_{\theta,d}(n)\mathbf{k}_n. \quad (2)$$

This approach enhances the model’s ability to capture relative positional relationships, improving its adaptability to diverse medical visual inputs.

Medical Instruction-Following Tuning. In stage 2, we make all model parameters trainable to improve the model’s capability in following complex textual instructions based on visual inputs.

We train the model using 647K instruction-answer pairs from PubMedVision_SFT (Chen et al., 2024). Both stage 1 and stage 2 focus on 2D images, as our experiments indicate that a strong foundational understanding of 2D images is crucial to extend Med-VLMs to complex 3D images and videos. By the end of this stage, the model can effectively handle various visual tasks related to 2D images.

Medical Mixed-Modal Tuning. In stage 3, the

goal is to expand the model’s capabilities from 2D images to 3D images (spatial) and videos (temporal). However, processing 3D images and videos is computationally expensive. In response, we introduce a token pruning mechanism to remove redundant information while preserving critical content. We found that consecutive slices in 3D medical images and adjacent frames in medical videos often contain repetitive or similar information. Hence, we compressed visual tokens by calculating the $L1$ distance between patches of consecutive views or frames. Tokens with an $L1$ distance below a threshold of 0.1 are identified as redundant and removed. This pruning method effectively reduces unnecessary visual data without impacting model performance. The model is trained with all 252K samples in OmniV-Med-Instruct with a standard autoregressive loss. All parameters are trainable to fully unleash the model’s potential, enabling it to extrapolate visual understanding to spatiotemporal dimensions and enhance downstream performance across diverse tasks. Our approach achieves SoTA accuracy with improved efficiency, enhancing its practicality for real-world medical tasks.

3 Experiment

3.1 Settings

We comprehensively evaluate OmniV-Med on seven medical benchmarks covering 2D/3D and video QA tasks. For 2D images, we follow LLaVA-Med and measure accuracy and recall on Rad-VQA (Lau et al., 2018), SLAKE (Liu et al., 2021), and PathVQA (He et al., 2020). For 3D images, we evaluate on M3D-VQA tasks (Bai et al., 2024) with metrics consistent with previous studies. For videos, we report the accuracy on Cholec80-VQA (Seenivasan et al., 2022), PSI-AVA-VQA (Valderrama et al., 2022), and EndoVis18-VQA (Seenivasan et al., 2023).

We compare OmniV-Med against domain-specific SoTA baselines across medical 2D/3D and video tasks. For 2D images, we select Med-MoE (Jiang et al., 2024d), LLaVA-Med (Li et al., 2024b), and BiomedGPT (Zhang et al., 2023a) as baselines. For 3D images, we compare with RadFM (Wu et al., 2023a) and M3D-LaMed (Bai et al., 2024). In the video domain, we compare against Surgical-VQA (Seenivasan et al., 2022), LV-GPT (Seenivasan et al., 2023) and Surgical-LLaVA (Jin and Jeong, 2024b).

3.2 Main Results

Consistent Improvements over all Modalities and Tasks. Our experiments demonstrate that OmniV-Med achieves superior performance than modality-specific SoTA baselines across all benchmarks and modalities, highlighting the strong generalization capability. Additionally, our token pruning strategy significantly reduces the number of tokens by an average of 60% for 3D images and medical videos, substantially lowering training and inference costs. This also enables support for long-video inference (see Figure 9), further demonstrate the universal capability of OmniV-Med.

3.3 Ablation Study and Analysis

Ablation of Arbitrary Resolutions. To validate the effectiveness of 2D rotary position embeddings (RoPE) in learning relationships between image patches, we conducted experiments by replacing fixed position embeddings with RoPE while keeping the visual encoder unchanged. As shown in Table 4, using the same data in Stage 1 and Stage 2, and training only on 2D images in Stage 3, we found that RoPE better captures relative positional relationships between patches, significantly improving performance on 2D tasks.

Ablation of Medical-Aware Token Reduction. We conduct experiments to evaluate the impact of token reduction on performance and computational cost. As shown in Figure 6, the incorporation of token reduction significantly reduces visual tokens for 3D images and videos by an average of 60%. More importantly, this pruning strategy, which leverages the characteristics of medical images, does not degrade performance. Instead, it helps the model focus on more critical regions of the images, leading to improved performance.

Cost Analysis. Training the OmniV-Med-1.5B model requires less than 24GB of GPU memory, due to our high-quality data, unified visual encoder, and medical-aware token reduction method. This enables training on eight RTX 3090 GPUs, while the 7B version supports inference on a single RTX 3090 GPU. Such efficiency enhances accessibility and underscores the practical value of our models for real-world clinical applications.

Unified Visual Understanding Enables Task Transferring Capability. Our analysis reveals that by employing 2D RoPE, the model learns the relative positional relationships between patches in 2D medical images, which extends to under-

Method	VQA-RAD		SLAKE		PathVQA	
	Open	Closed	Open	Closed	Open	Closed
<i>Representative & SoTA methods with numbers reported in the literature (Non-VLM Based Methods)</i>						
VL Encoder–Decoder (Bazi et al., 2023)	-	82.47	-	-	-	85.61
Q2ATransformer (Liu et al., 2023)	-	81.20	-	-	54.85	88.85
Prefix T. Medical LM (van Sonsbeek et al., 2023)	-	-	-	82.01	-	87.00
PubMedCLIP (Eslami et al., 2023)	-	80.00	-	82.50	-	-
BiomedCLIP (Zhang et al., 2023b)	-	79.80	-	89.70	-	-
M2I2 (Li et al., 2022)	-	83.50	-	91.10	-	88.00
BiomedGPT-S (Zhang et al., 2023a)	13.40	57.80	66.50	73.30	10.70	84.20
BiomedGPT-M (Zhang et al., 2023a)	53.60	65.07	78.30	86.80	12.5	85.70
CLIP-ViT w/ GPT2-XL	-	-	84.30	82.10	40.0	87.00
<i>Results (VLM Based Methods)</i>						
LLaVA (Liu et al., 2024a)	50.00	65.07	78.18	63.22	7.74	63.20
Med-Flamingo (Moor et al., 2023a)	50.00	65.07	78.18	63.22	7.74	63.20
HuatuoGPT-Vision-34B (Chen et al., 2024)	-	63.80	-	74.50	-	59.90
LLaVA-Med (LLama7B) (Li et al., 2024b)	61.52	84.19	83.08	85.34	37.95	91.21
LLaVA-Med (Vicuna7B) (Li et al., 2024b)	<u>64.39</u>	81.98	84.71	83.17	38.87	91.65
Med-MoE (Phi2-3.6B) (Jiang et al., 2024d)	58.55	82.72	<u>85.06</u>	85.58	34.74	91.98
Med-MoE (StableLM-2B) (Jiang et al., 2024d)	50.08	80.07	83.16	83.41	33.79	91.30
OmniV-Med-Tiny (Qwen2.5-1.5B)	59.22	<u>84.93</u>	84.59	<u>87.98</u>	<u>38.87</u>	<u>92.66</u>
OmniV-Med (Qwen2.5-7B)	67.87	88.24	85.92	91.51	41.68	93.42

Table 1: Performance on Med-VQA tasks. **Bold** denotes the best performance; underlined denotes the second-best.

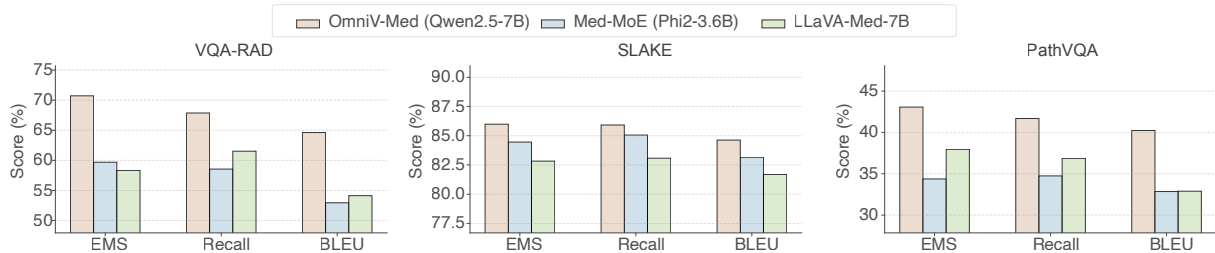


Figure 5: Detailed comparison with additional metrics in open settings. EMS denotes *Exact Match Score*.

Methods	Plane	Phase	Organ	Abnormality	Location	Avg.
Closed-End (Accuracy)						
RadFM (Wu et al., 2023a)	19.65	28.70	16.80	18.92	14.88	19.79
M3D-LaMed (Bai et al., 2024)	98.80	79.75	74.75	66.65	58.94	75.78
OmniV-Med-Tiny (Qwen2.5-1.5B)	98.95	<u>91.35</u>	<u>75.15</u>	66.24	<u>60.78</u>	<u>78.49</u>
OmniV-Med (Qwen2.5-7B)	98.75	91.65	76.35	66.80	61.86	79.08
Open-End (Recall)						
RadFM (Wu et al., 2023a)	14.24	14.25	14.24	15.64	23.58	16.39
M3D-LaMed-7B (Bai et al., 2024)	<u>98.37</u>	74.41	34.20	15.91	24.00	49.38
OmniV-Med-Tiny (Qwen2.5-1.5B)	98.18	88.80	<u>40.62</u>	<u>16.80</u>	<u>26.04</u>	<u>54.09</u>
OmniV-Med (Qwen2.5-7B)	98.84	<u>86.70</u>	41.36	17.26	26.75	54.18

Table 2: Performance Comparison of Methods in M3D Tasks.

standing patches across multi-view (3D) and multi-time (video) dimensions. Specifically, even without video-specific training data during stage 1 and stage 2, OmniV-Med demonstrates exceptional comprehension of video content. As shown in Figure 8, the model accurately interprets complex medical

surgical procedures, highlighting significant improvements over traditional ViT-based approaches.

Effect of Data Scaling. By incorporating diverse modalities in stage 3 on a unified visual encoder, we observe that introducing 3D images and videos alongside 2D images does not degrade performance

Methods	Cholec80-VQA	EndoVis18-VQA	PSI-AVA-VQA
VisualBert (Li et al., 2019)	89.7	61.4	58.5
Block (Ben-Younes et al., 2019)	89.5	60.1	59.9
MFH (Yu et al., 2018)	87.5	58.8	47.8
Surgical-VQA (Seenivasan et al., 2022)	89.8	63.2	65.6
LV-GPT (Seenivasan et al., 2023)	87.5	68.1	59.3
Surgical-LLaVA (Jin and Jeong, 2024a)	<u>92.2</u>	68.7	<u>67.1</u>
OmniV-Med-Tiny (Qwen2.5-1.5B)	91.7	<u>78.8</u>	64.8
OmniV-Med (Qwen2.5-7B)	92.9	80.3	69.3

Table 3: Performance Comparison of Methods on Different Video Benchmarks.

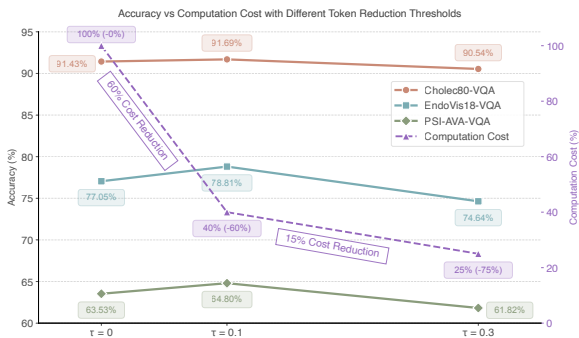


Figure 6: Ablation study on token reduction threshold and cost comparison (Further results in Table 5).

on 2D benchmarks. Instead, it enhances performance, as shown in Figure 10. This indicates that our training paradigm enables Med-VLMs to follow the data scaling law (Kaplan et al., 2020) in multimodal training scenarios, where increasing training data consistently improves performance.

Progressive Training Yields the Best Performance. We investigate the effect of jointly training stage 2 (2D images) and stage 3 (mixed-modal data) compared to our progressive training strategy. As shown in Table 11, the best performance is achieved when 2D image understanding is robustly established before extending to 3D images and videos. This underscores the importance of 2D image understanding as a foundation and validates the effectiveness of our progressive strategy.

Effect of Task Transferring Capability We conducted a zero-shot Video-VQA (Video Question Answering) capability comparison between OmniV-Med, trained only on 2D images through stages 1 and 2, and LLaVA-Med-LLaMA3.2 (Li et al., 2024b), which has demonstrated excellent performance in 2D images. We selected a total of 120 original VQA items from Cholec80-VQA (Seenivasan et al., 2022),

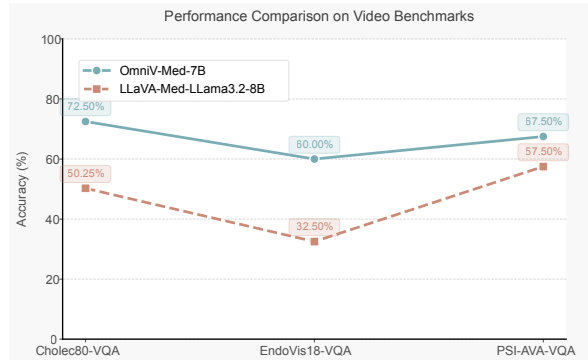


Figure 7: Task transferring capability of OmniV-Med.

PSI-AVA-VQA (Valderrama et al., 2022), and EndoVis18-VQA (Seenivasan et al., 2023), and reformulated them into multiple-choice questions where the model selects "yes" or "no" to evaluate its zero-shot VQA performance. As shown in Figure 7, our OmniV-Med exhibited superior task transfer capability, with its rotary position-adaptive encoder demonstrating exceptional generalization ability.

3.4 Related Work

Medical Large Vision-Language Models Following the success of general-purpose Vision-Language Models (VLMs) (Jiang et al., 2024a,b; Li et al., 2024a; Zhang et al., 2025), recent advancements in Medical Large Vision-Language Models have showcased specialized paradigms tailored for 2D, 3D, and video-based medical imaging (Liu et al., 2024b; Wu et al., 2023b). For 2D imaging, models like LLaVA-Med (Li et al., 2024b) leverage multi-stage training (pretraining-modality alignment-fine-tuning) to align X-rays with diagnostic reports, while Med-MoE (Jiang et al., 2024d) employs mixture-of-experts architectures to balance computational efficiency and diagnostic accuracy. In 3D imaging, M3D-LaMed (Bai et al.,

Embedding Type	Model	VQA-RAD		SLAKE		PathVQA	
		Recall	Accuracy	Recall	Accuracy	Recall	Accuracy
Fixed Positional Embedding	OmniV-Med-Tiny	55.50	82.93	80.23	83.12	33.26	90.19
Rotary Position Embedding	OmniV-Med-Tiny	59.22 (+3.72)	84.93 (+2.00)	84.59 (+4.36)	87.98 (+4.86)	38.87 (+5.61)	92.66 (+2.47)

Table 4: Ablation of Fixed Positional Embedding and Rotary Position Embedding.

Threshold & Method		Cholec80-VQA	EndoVis18-VQA	PSI-AVA-VQA
0	OmniV-Med-Tiny	91.43	77.05	63.53
0.1	OmniV-Med-Tiny	91.69 (+0.26)	78.81 (+1.76)	64.80 (+1.27)
0.3	OmniV-Med-Tiny	90.54	74.64	61.82

Table 5: Performance Comparison on Video Datasets with Varying Token Reduction Thresholds.

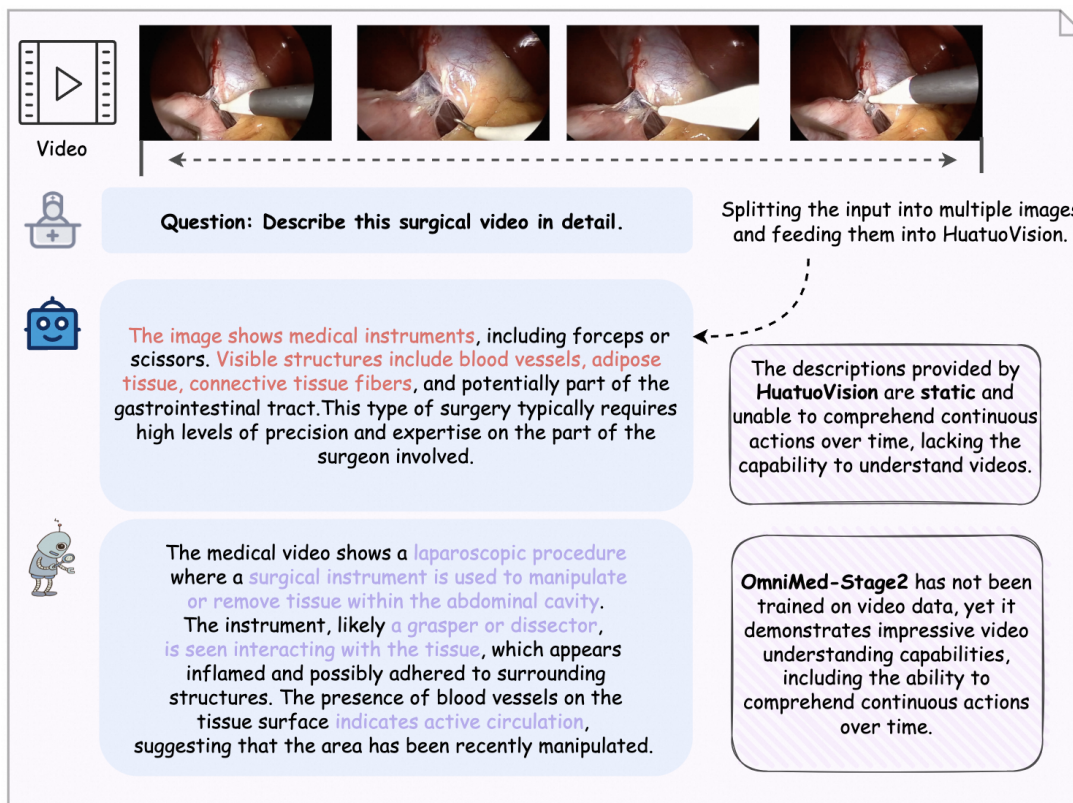


Figure 8: OmniV-Med-Stage2 demonstrates outstanding task transfer capability, extending from 2D image understanding to video comprehension, showcasing a strong grasp of temporal action dynamics.

2024) addresses volumetric complexity through 3D Vision Transformers and spatial pooling perceptrons, enabling cross-modal retrieval across CT/MRI datasets. RadFM (Wu et al., 2023b) further pioneers multi-modal integration, combining natural language queries with 2D/3D radiologic images via adaptive fusion mechanisms. For surgical video analysis, frameworks like Surgical-

LLaVA (Jin and Jeong, 2024a) are designed to handle surgical videos, providing real-time analysis and assistance during surgical procedures. Nevertheless, these methodologies possess inherent limitations: most models are restricted to unimodal visual analysis (e.g., X-ray or CT), lacking integration for multimodal diagnostic scenarios (e.g., 2D, 3D, Video). Single modality leads to inadequate

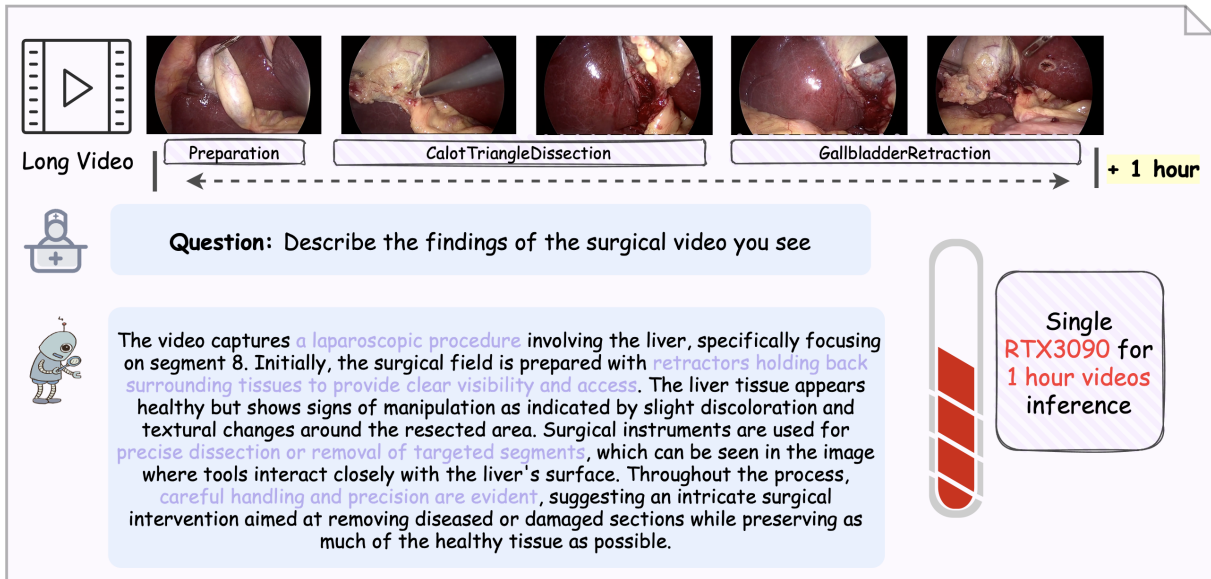


Figure 9: OmniV-Med demonstrates robust performance on long-video inference with one single RTX 3090.

cross-modal feature integration, while traditional architectures struggle to balance computational efficiency with anatomical detail preservation when handling high-resolution medical imaging (Yang et al., 2024).

4 Conclusion

In this paper, we construct the first multimodal instruction-following dataset containing 252K examples and train the OmniV-Med family of models, which includes two parameter sizes: 1.5B and 7B. These models are designed to flexibly support a wide range of practical clinical application scenarios. The OmniV-Med models achieve robust performance across diverse tasks involving 2D images, 3D volumes, and videos, demonstrating their versatility and effectiveness. Our work lays a solid foundation for the future development and practical deployment of Med-VLMs, paving the way for broader applications in clinical settings.

Ethical Considerations

In this study, we design a vision-language model with the potential for practical deployment in the medical domain, supporting multiple modalities of medical input, including 2D images, 3D volumes, and videos. Our work is grounded in the use of publicly available datasets that have been released by prior researchers, ensuring compliance with ethical standards. Specifically, all 2D and 3D images, as well as video data, are sourced from publicly accessible repositories and do not involve sensitive

personal information or privacy concerns.

To further ensure ethical integrity, the dataset entries have been manually checked to verify that they do not contain any content that could raise ethical or privacy issues. While our research leverages these well-established and pre-processed datasets, we recognize the importance of applying strict ethical considerations when extending our findings to other datasets, particularly those involving sensitive or private medical information. Robust safeguards must be implemented to protect patient confidentiality and prevent misuse of such data.

Additionally, as we advance the capabilities of vision-language models in the medical domain, it is crucial to balance these technological innovations with a careful assessment of their broader implications. This includes addressing potential challenges such as increased computational demands and their associated environmental impact, as well as ensuring equitable access to the benefits of these models across diverse healthcare settings.

References

Seongsu Bae, Daeun Kyung, Jaehee Ryu, Eunbyeol Cho, Gyubok Lee, Sunjun Kweon, Jungwoo Oh, Lei Ji, Eric Chang, Tackeun Kim, et al. 2024. Mimi-ext-mimic-cxr-vqa: A complex, diverse, and large-scale visual question answering dataset for chest x-ray images.

Fan Bai, Yuxin Du, Tiejun Huang, Max Q-H Meng, and Bo Zhao. 2024. M3d: Advancing 3d medical image analysis with multi-modal large language models. *arXiv preprint arXiv:2404.00578*.

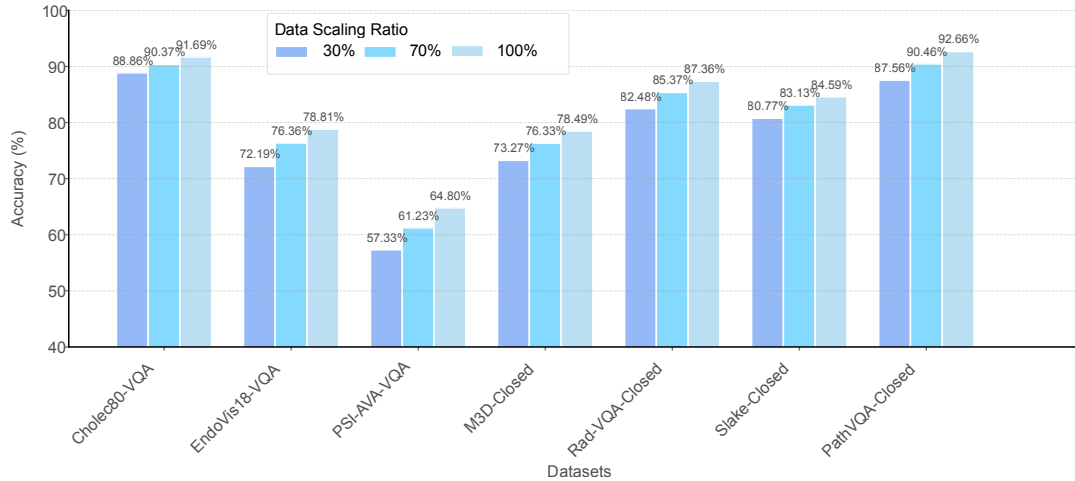


Figure 10: Performance under different data scaling ratio.

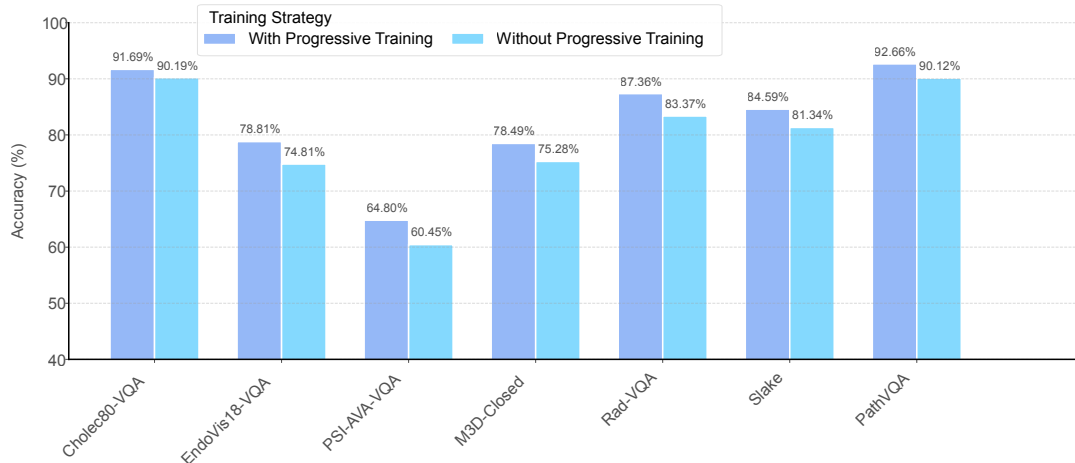


Figure 11: Performance comparison with and without progressive training strategy.

Jinze Bai, Shuai Bai, Shusheng Yang, Shijie Wang, Sinan Tan, Peng Wang, Junyang Lin, Chang Zhou, and Jingren Zhou. 2023. Qwen-vl: A frontier large vision-language model with versatile abilities. *arXiv preprint arXiv:2308.12966*.

Shuai Bai, Keqin Chen, Xuejing Liu, Jialin Wang, Wenbin Ge, Sibao Song, Kai Dang, Peng Wang, Shijie Wang, Jun Tang, et al. 2025. Qwen2. 5-vl technical report. *arXiv preprint arXiv:2502.13923*.

Yakoub Bazi, Mohamad Mahmoud Al Rahhal, Laila Bashmal, and Mansour Zuair. 2023. Vision-language model for visual question answering in medical imagery. *Bioengineering*.

Hedi Ben-Younes, Remi Cadene, Nicolas Thome, and Matthieu Cord. 2019. Block: Bilinear superdiagonal fusion for visual question answering and visual relationship detection. In *Proceedings of the AAAI conference on artificial intelligence*, volume 33, pages 8102–8109.

Sebastian Bodenstedt, Martin Wagner, Beat Peter

Müller-Stich, Jürgen Weitz, and Stefanie Speidel. 2020. Artificial intelligence-assisted surgery: potential and challenges. *Visceral Medicine*, 36(6):450–455.

Florian Bordes, Richard Yuanzhe Pang, Anurag Ajay, Alexander C. Li, Adrien Bardes, Suzanne Petryk, Oscar Mañas, Zhiqiu Lin, Anas Mahmoud, Bargav Jayaraman, Mark Ibrahim, Melissa Hall, Yunyang Xiong, Jonathan Lebensold, Candace Ross, Srihari Jayakumar, Chuan Guo, Diane Bouchacourt, Haider Al-Tahan, Karthik Padthe, Vasu Sharma, Hu Xu, Xiaoqing Ellen Tan, Megan Richards, Samuel Lavoie, Pietro Astolfi, Reyhane Askari Hemmat, Jun Chen, Kushal Tirumala, Rim Assouel, Mazda Moayeri, Arjang Talattof, Kamalika Chaudhuri, Zechun Liu, Xilun Chen, Quentin Garrido, Karen Ullrich, Aishwarya Agrawal, Kate Saenko, Asli Celikyilmaz, and Vikas Chandra. 2024. [An introduction to vision-language modeling](#). *Preprint*, arXiv:2405.17247.

Junying Chen, Chi Gui, Ruyi Ouyang, Anningzhe Gao, Shunian Chen, Guiming Hardy Chen, Xidong Wang,

- Ruifei Zhang, Zhenyang Cai, Ke Ji, et al. 2024. Huatuoogpt-vision, towards injecting medical visual knowledge into multimodal llms at scale. *arXiv preprint arXiv:2406.19280*.
- Rohan Choudhury, Guanglei Zhu, Sihan Liu, Koichiro Niinuma, Kris Kitani, and László Jeni. 2024. Don't look twice: Faster video transformers with run-length tokenization. *Advances in Neural Information Processing Systems*, 37:28127–28149.
- Mostafa Dehghani, Basil Mustafa, Josip Djolonga, Jonathan Heek, Matthias Minderer, Mathilde Caron, Andreas Steiner, Joan Puigcerver, Robert Geirhos, Ibrahim M Alabdulmohsin, et al. 2023. Patch n'pack: Navit, a vision transformer for any aspect ratio and resolution. *Advances in Neural Information Processing Systems*, 36:2252–2274.
- Sedigheh Eslami, Christoph Meinel, and Gerard De Melo. 2023. Pubmedclip: How much does clip benefit visual question answering in the medical domain? In *Findings of the Association for Computational Linguistics: EACL 2023*, pages 1151–1163.
- Xiaoxuan He, Yifan Yang, Xinyang Jiang, Xufang Luo, Haoji Hu, Siyun Zhao, Dongsheng Li, Yuqing Yang, and Lili Qiu. 2024. Unified medical image pre-training in language-guided common semantic space. In *European Conference on Computer Vision*, pages 123–139. Springer.
- Xuehai He, Yichen Zhang, Luntian Mou, Eric Xing, and Pengtao Xie. 2020. Pathvqa: 30000+ questions for medical visual question answering. *arXiv preprint arXiv:2003.10286*.
- Roy Hirsch, Mathilde Caron, Regev Cohen, Amir Livne, Ron Shapiro, Tomer Golany, Roman Goldenberg, Daniel Freedman, and Ehud Rivlin. 2023. Self-supervised learning for endoscopic video analysis. In *International Conference on Medical Image Computing and Computer-Assisted Intervention*, pages 569–578. Springer.
- Songtao Jiang, Yan Zhang, Ruizhe Chen, Yeying Jin, and Zuozhu Liu. 2024a. Modality-fair preference optimization for trustworthy mllm alignment. *arXiv preprint arXiv:2410.15334*.
- Songtao Jiang, Yan Zhang, Chenyi Zhou, Yeying Jin, Yang Feng, Jian Wu, and Zuozhu Liu. 2024b. Joint visual and text prompting for improved object-centric perception with multimodal large language models. *arXiv preprint arXiv:2404.04514*.
- Songtao Jiang, Tuo Zheng, Yan Zhang, Yeying Jin, Li Yuan, and Zuozhu Liu. 2024c. Med-moe: Mixture of domain-specific experts for lightweight medical vision-language models. In *Conference on Empirical Methods in Natural Language Processing*.
- Songtao Jiang, Tuo Zheng, Yan Zhang, Yeying Jin, Li Yuan, and Zuozhu Liu. 2024d. Med-moe: Mixture of domain-specific experts for lightweight medical vision-language models. In *Findings of the Association for Computational Linguistics: EMNLP 2024*, pages 3843–3860.
- Jing Jiao, Jin Zhou, Xiaokang Li, Menghua Xia, Yi Huang, Lihong Huang, Na Wang, Xiaofan Zhang, Shichong Zhou, Yuanyuan Wang, and Yi Guo. 2023. Usfm: A universal ultrasound foundation model generalized to tasks and organs towards label efficient image analysis. *Medical image analysis*, 96:103202.
- Juseong Jin and Chang Wook Jeong. 2024a. Surgical-llava: Toward surgical scenario understanding via large language and vision models. *Preprint, arXiv:2410.09750*.
- Juseong Jin and Chang Wook Jeong. 2024b. Surgical-llava: Toward surgical scenario understanding via large language and vision models. *arXiv preprint arXiv:2410.09750*.
- Jared Kaplan, Sam McCandlish, Tom Henighan, Tom B Brown, Benjamin Chess, Rewon Child, Scott Gray, Alec Radford, Jeffrey Wu, and Dario Amodei. 2020. Scaling laws for neural language models. *arXiv preprint arXiv:2001.08361*.
- Earl J Kirkland and Earl J Kirkland. 2010. Bilinear interpolation. *Advanced computing in electron microscopy*, pages 261–263.
- Jason J Lau, Soumya Gayen, Asma Ben Abacha, and Dina Demner-Fushman. 2018. A dataset of clinically generated visual questions and answers about radiology images. *Scientific data*, 5(1):1–10.
- Bo Li, Yuanhan Zhang, Dong Guo, Renrui Zhang, Feng Li, Hao Zhang, Kaichen Zhang, Peiyuan Zhang, Yanwei Li, Ziwei Liu, et al. 2024a. Llava-onevision: Easy visual task transfer. *arXiv preprint arXiv:2408.03326*.
- Chunyuan Li, Cliff Wong, Sheng Zhang, Naoto Usuyama, Haotian Liu, Jianwei Yang, Tristan Naumann, Hoifung Poon, and Jianfeng Gao. 2024b. Llava-med: Training a large language-and-vision assistant for biomedicine in one day. *Advances in Neural Information Processing Systems*, 36.
- Feng Li, Renrui Zhang, Hao Zhang, Yuanhan Zhang, Bo Li, Wei Li, Zejun Ma, and Chunyuan Li. 2024c. Llava-next-interleave: Tackling multi-image, video, and 3d in large multimodal models. *Preprint, arXiv:2407.07895*.
- KunChang Li, Yinan He, Yi Wang, Yizhuo Li, Wenhui Wang, Ping Luo, Yali Wang, Limin Wang, and Yu Qiao. 2023. Videochat: Chat-centric video understanding. *arXiv preprint arXiv:2305.06355*.
- Liunian Harold Li, Mark Yatskar, Da Yin, Cho-Jui Hsieh, and Kai-Wei Chang. 2019. Visualbert: A simple and performant baseline for vision and language. *arXiv preprint arXiv:1908.03557*.

- Pengfei Li, Gang Liu, Lin Tan, Jinying Liao, and Shenjun Zhong. 2022. Self-supervised vision-language pretraining for medical visual question answering. *arXiv preprint arXiv:2211.13594*.
- Bin Lin, Yang Ye, Bin Zhu, Jiayi Cui, Munan Ning, Peng Jin, and Li Yuan. 2023. Video-llava: Learning united visual representation by alignment before projection. *arXiv preprint arXiv:2311.10122*.
- Bo Liu, Li-Ming Zhan, Li Xu, Lin Ma, Yan Yang, and Xiao-Ming Wu. 2021. Slake: A semantically-labeled knowledge-enhanced dataset for medical visual question answering. In *2021 IEEE 18th International Symposium on Biomedical Imaging (ISBI)*, pages 1650–1654. IEEE.
- Haotian Liu, Chunyuan Li, Yuheng Li, and Yong Jae Lee. 2024a. Improved baselines with visual instruction tuning. In *Proceedings of the IEEE/CVF Conference on Computer Vision and Pattern Recognition (CVPR)*, pages 26296–26306.
- Jiaxiang Liu, Yuan Wang, Jiawei Du, Joey Tianyi Zhou, and Zuozhu Liu. 2024b. [Medcot: Medical chain of thought via hierarchical expert](#). *Preprint*, arXiv:2412.13736.
- Yunyi Liu, Zhanyu Wang, Dong Xu, and Luping Zhou. 2023. Q2atransformer: Improving medical vqa via an answer querying decoder. *arXiv preprint arXiv:2304.01611*.
- Ming Y. Lu, Bowen Chen, Drew F. K. Williamson, Richard J. Chen, Melissa Zhao, Aaron K Chow, Kenji Ikemura, Ahromg Kim, Dimitra Pouli, Ankush Patel, Amr Soliman, Chengkuan Chen, Tong Ding, Judy J. Wang, Georg K. Gerber, Ivy Liang, Long Phi Le, Anil V. Parwani, Luca L Weishaupt, and Faisal Mahmood. 2024. [A multimodal generative ai copilot for human pathology](#). *Nature*, 634:466 – 473.
- Michael Moor, Qian Huang, Shirley Wu, Michihiro Yasunaga, Yash Dalmia, Jure Leskovec, Cyril Zakka, Eduardo Pontes Reis, and Pranav Rajpurkar. 2023a. Med-flamingo: a multimodal medical few-shot learner. In *Machine Learning for Health (ML4H)*, pages 353–367. PMLR.
- Michael Moor, Qian Huang, Shirley Wu, Michihiro Yasunaga, Cyril Zakka, Yashodhara Dalmia, Eduardo Pontes Reis, Pranav Rajpurkar, and Jure Leskovec. 2023b. [Med-flamingo: a multimodal medical few-shot learner](#). *ArXiv*, abs/2307.15189.
- Chinedu Innocent Nwoye, Deepak Alapatt, Tong Yu, Armine Vardazaryan, Fangfang Xia, Zixuan Zhao, Tong Xia, Fucang Jia, Yuxuan Yang, Hao Wang, et al. 2023. Cholectriplet2021: A benchmark challenge for surgical action triplet recognition. *Medical Image Analysis*, 86:102803.
- Alec Radford, Jong Wook Kim, Chris Hallacy, Aditya Ramesh, Gabriel Goh, Sandhini Agarwal, Girish Sastry, Amanda Askell, Pamela Mishkin, Jack Clark, et al. 2021. Learning transferable visual models from natural language supervision. In *International conference on machine learning*, pages 8748–8763. PMLR.
- Sucheng Ren, Xiaoke Huang, Xianhang Li, Junfei Xiao, Jieru Mei, Zeyu Wang, Alan Yuille, and Yuyin Zhou. 2024. Medical vision generalist: Unifying medical imaging tasks in context. *arXiv preprint arXiv:2406.05565*.
- Lalithkumar Seenivasan, Mobarakol Islam, Gokul Kannan, and Hongliang Ren. 2023. Surgicalgpt: end-to-end language-vision gpt for visual question answering in surgery. In *International conference on medical image computing and computer-assisted intervention*, pages 281–290. Springer.
- Lalithkumar Seenivasan, Mobarakol Islam, Adithya K Krishna, and Hongliang Ren. 2022. Surgical-vqa: Visual question answering in surgical scenes using transformer. In *International Conference on Medical Image Computing and Computer-Assisted Intervention*, pages 33–43. Springer.
- Hugo Touvron, Louis Martin, Kevin Stone, Peter Albert, Amjad Almahairi, Yasmine Babaei, Nikolay Bashlykov, Soumya Batra, Prajjwal Bhargava, Shrutu Bhosale, et al. 2023. Llama 2: Open foundation and fine-tuned chat models. *arXiv preprint arXiv:2307.09288*.
- Natalia Valderrama, Paola Ruiz Puentes, Isabela Hernández, Nicolás Ayobi, Mathilde Verlyck, Jessica Santander, Juan Caicedo, Nicolás Fernández, and Pablo Arbeláez. 2022. Towards holistic surgical scene understanding. In *International conference on medical image computing and computer-assisted intervention*, pages 442–452. Springer.
- Tom van Sonsbeek, Mohammad Mahdi Derakhshani, Ivona Najdenkoska, Cees GM Snoek, and Marcel Worring. 2023. Open-ended medical visual question answering through prefix tuning of language models. *arXiv preprint arXiv:2303.05977*.
- Risheng Wang, Tao Lei, Ruixia Cui, Bingtao Zhang, Hongying Meng, and Asoke K Nandi. 2022. Medical image segmentation using deep learning: A survey. *IET image processing*, 16(5):1243–1267.
- Zhao Wang, Chang Liu, Shaoting Zhang, and Qi Dou. 2023. Foundation model for endoscopy video analysis via large-scale self-supervised pre-train. In *International Conference on Medical Image Computing and Computer-Assisted Intervention*, pages 101–111. Springer.
- Chaoyi Wu, Xiaoman Zhang, Ya Zhang, Yanfeng Wang, and Weidi Xie. 2023a. Towards generalist foundation model for radiology by leveraging web-scale 2d&3d medical data. *arXiv preprint arXiv:2308.02463*.
- Chaoyi Wu, Xiaoman Zhang, Ya Zhang, Yanfeng Wang, and Weidi Xie. 2023b. [Towards generalist foundation model for radiology by leveraging web-scale 2d&3d medical data](#). *Preprint*, arXiv:2308.02463.

- Shengqiong Wu, Hao Fei, Leigang Qu, Wei Ji, and Tat-Seng Chua. 2023c. [Next-gpt: Any-to-any multimodal llm](#). *ArXiv*, abs/2309.05519.
- Shengqiong Wu, Hao Fei, Leigang Qu, Wei Ji, and Tat-Seng Chua. 2024. [Next-gpt: Any-to-any multimodal llm](#). In *Forty-first International Conference on Machine Learning*.
- Hanwen Xu, Naoto Usuyama, Jaspreet Bagga, Sheng Zhang, Rajesh Rao, Tristan Naumann, Cliff Wong, Zelalem Gero, Javier González, Yu Gu, Yanbo Xu, Mu-Hsin Wei, Wenhui Wang, Shuming Ma, Furu Wei, Jianwei Yang, Chun yue Li, Jianfeng Gao, Jaylen Rosemon, Tucker Bower, Soohee Lee, Roshanthi K. Weerasinghe, Bill J Wright, Ari Robicsek, Brian D. Piening, Carlo Bifulco, Sheng Wang, and Hoifung Poon. 2024. [A whole-slide foundation model for digital pathology from real-world data](#). *Nature*, 630:181 – 188.
- Mingjing Yang, Zhicheng Wu, Hanyu Zheng, Liqin Huang, Wangbin Ding, Lin Pan, and Lei Yin. 2024. [Cross-modality medical image segmentation via enhanced feature alignment and cross pseudo supervision learning](#). *Diagnostics*, 14(16):1751.
- Zhou Yu, Jun Yu, Chenchao Xiang, Jianping Fan, and Dacheng Tao. 2018. [Beyond bilinear: Generalized multimodal factorized high-order pooling for visual question answering](#). *IEEE transactions on neural networks and learning systems*, 29(12):5947–5959.
- Xiaohua Zhai, Basil Mustafa, Alexander Kolesnikov, and Lucas Beyer. 2023. [Sigmoid loss for language image pre-training](#). In *Proceedings of the IEEE/CVF international conference on computer vision*, pages 11975–11986.
- Jun Zhan, Junqi Dai, Jiasheng Ye, Yunhua Zhou, Dong Zhang, Zhigeng Liu, Xin Zhang, Ruibin Yuan, Ge Zhang, Linyang Li, Hang Yan, Jie Fu, Tao Gui, Tianxiang Sun, Yugang Jiang, and Xipeng Qiu. 2024a. [Anygpt: Unified multimodal llm with discrete sequence modeling](#). In *Annual Meeting of the Association for Computational Linguistics*.
- Jun Zhan, Junqi Dai, Jiasheng Ye, Yunhua Zhou, Dong Zhang, Zhigeng Liu, Xin Zhang, Ruibin Yuan, Ge Zhang, Linyang Li, et al. 2024b. [Anygpt: Unified multimodal llm with discrete sequence modeling](#). *arXiv preprint arXiv:2402.12226*.
- Boqiang Zhang, Kehan Li, Zesen Cheng, Zhiqiang Hu, Yuqian Yuan, Guanzheng Chen, Sicong Leng, Yuming Jiang, Hang Zhang, Xin Li, et al. 2025. [Videollama 3: Frontier multimodal foundation models for image and video understanding](#). *arXiv preprint arXiv:2501.13106*.
- Kai Zhang, Jun Yu, Zhiling Yan, Yixin Liu, Eashan Adhikarla, Sunyang Fu, Xun Chen, Chen Chen, Yuyin Zhou, Xiang Li, et al. 2023a. [Biomedgpt: A unified and generalist biomedical generative pre-trained transformer for vision, language, and multimodal tasks](#). *arXiv preprint arXiv:2305.17100*.
- Kai Zhang, Rong Zhou, Eashan Adhikarla, Zhiling Yan, Yixin Liu, Jun Yu, Zhengliang Liu, Xun Chen, Brian D Davison, Hui Ren, et al. 2024. [A generalist vision–language foundation model for diverse biomedical tasks](#). *Nature Medicine*, pages 1–13.
- Sheng Zhang, Yanbo Xu, Naoto Usuyama, Jaspreet Bagga, Robert Tinn, Sam Preston, Rajesh Rao, Mu Wei, Naveen Valluri, Cliff Wong, et al. 2023b. [Large-scale domain-specific pretraining for biomedical vision-language processing](#). *arXiv preprint arXiv:2303.00915*.
- Yukun Zhou, Mark A. Chia, Siegfried K. Wagner, Murat S. Ayhan, Dominic J. Williamson, Robert R. Struyven, Timing Liu, Moucheng Xu, Matteo G. Lozano, Peter Woodward-Court, Yuka Kihara, Naomi John E. J. Thomas Tariq Paul Graeme Panagiotis Den Allen Gallacher Littlejohns Aslam Bishop Black Ser, Naomi Allen, John Gallacher, Thomas J Littlejohns, Tariq Aslam, Paul Bishop, Graeme Black, Panagiotis Sergouniotis, Denize Atan, Andrew D. Dick, Cathy Williams, Sarah Ann Barman, Jenny H. Barrett, Sarah Mackie, Tasanee Braithwaite, Roxana O. Carare, Sarah Ennis, Jane Gibson, Andrew J. Lotery, Jay Self, Usha Chakravarthy, Ruth E. Hogg, Euan Neil Paterson, Jayne Woodside, Tunde Peto, Gareth J. McKay, Bernadette Mcguinness, Paul J. Foster, Konstantinos Balaskas, Anthony P. Khawaja, Nikolas Pontikos, Jugnoo S. Rahi, Gerassimos Lascaratos, Praveen J. Patel, Michelle Chan, Sharon Y. L. Chua, Alexander Day, Parul Desai, Catherine A Egan, Marcus Fruttiger, David F. Garway-Heath, Alison Hardcastle, Sir Peng Tee Khaw, Tony Moore, Sobha Sivaprasad, Nicholas G. Strouthidis, Dhanes Thomas, Adnan Tufail, Ananth C. Viswanathan, Bal Dhillon, Tom Macgillivray, Cathie L. M. Sudlow, Véronique Vitar, Alexander Doney, Emanuele Trucco, Jeremy A. Guggenheim, James E. Morgan, Chris J. Hammond, Katie M. Williams, Pirro G. Hysi, Simon Harding, Yalin Zheng, Robert Luben, Phil Luthert, Zihan Sun, Martin McKibbin, Eoin O’sullivan, Richard Oram, Mike Weedon, Chris G. Owen, Alicja R. Rudnicka, Naveed Sattar, David Steel, Irene Stratton, Robyn Tapp, Max M. Yates, Axel Petzold, Savita Madhusudan, Andre Altmann, Aaron Y. Lee, Eric J. Topol, Alastair Keith Denniston, Daniel C Alexander, and Pearse Andrew Keane. 2023. [A foundation model for generalizable disease detection from retinal images](#). *Nature*, 622:156 – 163.